Final Project Report

Project Title:	High Altitude Radiation Detector (GU-HARD-PL02)
Institution:	Gannon University
Contact Author:	Dr. Wookwon Lee
	Dept. of Electrical and Computer Engineering
	Gannon University
	109 University Square, Erie, PA 16541
	Email: lee023@gannon.edu
Project Duration:	01/01/2012 – 12/14/2012
Date submitted:	12/14/2012

Table of Contents

1. Highlights of the Project 4
2. Payload Subsystems 5
   2.1. Detector Module 6
   2.2. Comparator Module 7
   2.3. Coincidence Detector 7
   2.4. Microprocessor/CPU 8
   2.5. Power Module 9
3. Numerical Results and Discussions 9
   3.1. Lab Testing Data – Detector and Comparator Modules 9
   3.2. In-Flight Experimental Data 10
4. Failure Mode and Effect Analysis 13
5. Participants 14
6. Presentations and Publications 15
7. Concluding Remarks 15
References 16

List of Figures

Figure 1. Overall functional block diagram for cosmic ray measurement 4
Figure 2. Completed, sealed GU-HARD-PL02 5
Figure 3. Setup for lab testing 5
Figure 4. Interior view of GU-HARD-PL02 6
Figure 5. Detector module: (a) photo diode and scintillator (b) integration with a preamplifier 6
Figure 6. Application circuit diagram of the pre-amplifier for SSPM [3] 7
Figure 7. Fully assembled detector module with the rotator module 7
Figure 8. Output signals: (a) pre-amplifier (b) OP amp (comparator) 10
Figure 9. Temperature inside the payload 11
Figure 10. Orientation angle [degrees] of the electronic compass referenced to the East-West 11
Figure 11. Number of coincidence events counted by the Coincidence Module 12
Figure 12. Coincidence rate [Events per minute] in all directions 12
Figure 13. Coincidence rate [Events per minute] in East-West direction 13

List of Tables

Table 1. Testing Data of the Detector Module 10

1. Highlights of the Project

Project Objectives – The Earth's magnetic field deflects cosmic-ray trajectories from a straight line. Due to the fact that cosmic rays are predominantly positively charged, this results in more particles arriving from the west than from the east. This "east-west" asymmetry has been investigated in the past at ground level. The goal of the proposed HASP2012 small payload was to investigate how the "east-west" angular asymmetry changes with altitude, as the cosmic ray flux transitions from mostly secondary particles near the ground level to mostly primary cosmic rays near balloon-float altitudes [1]. Additionally, this project intended to study how the intensity of cosmic rays changes with altitude, based on measurements of cosmic ray intensity from multiple arrival directions, providing a more complete picture of the high-altitude radiation environment caused by cosmic rays.

Payload Subsystems – To achieve the project goal, a payload integrating various subsystems for cosmic-ray detection and necessary processing has been designed in a top-down design approach: initially establishing engineering requirements of the payload for the experiment, carrying out functional decomposition, and actual laboratory design of subsystems by student team members from the Electrical

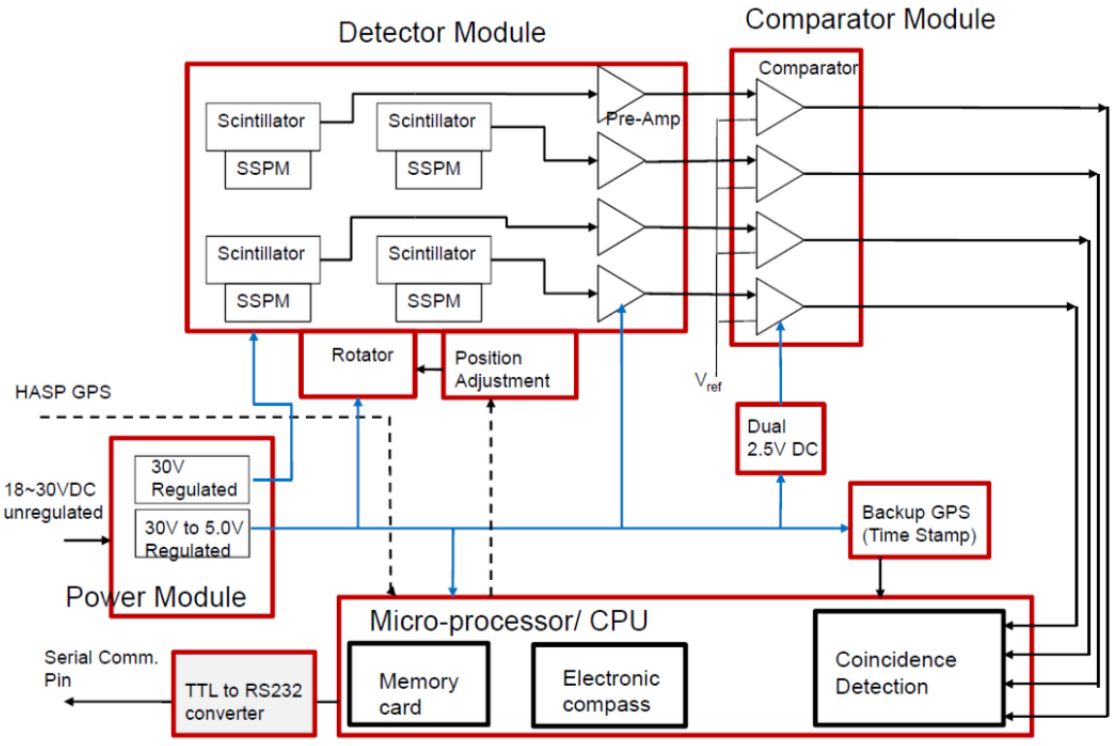

Figure 1. Overall functional block diagram for cosmic ray measurement

and Computer Engineering (ECE) department at Gannon. Figure 1 shows the functional block diagram of the payload for the experiment, and Figure 2 shows a completed, sealed payload waiting for thermal and vacuum testing at the CSBF site. Details of key subsystems and their performance during flight are described further in the following section.

Figure 2. Completed, sealed GU-HARD-PL02

Project Milestones and Deliverables – The team delivered all monthly status reports from January 2012 to November 2012 on design activities for payload subsystems, a Payload Specification & Integration Plan (PSIP), Flight Operation Plan (FLOP), and on-site payload integration at the CSBF lab, as well as post-balloon launch activities.

Participants – The student team consisted of a total of six ECE undergraduate students including three seniors and three sophomores, one graduate student, and two faculty advisors from ECE and Physics department.

2. Payload Subsystems

The key subsystems of the payload are the detector module, comparator module, coincidence detector, micro-processor/CPU, and power module. A brief description of each module is given below. A photo of the payload in the lab, prior to integration, is shown in Figure 3, and an exploded view of the payload after integration is shown in Figure 4.

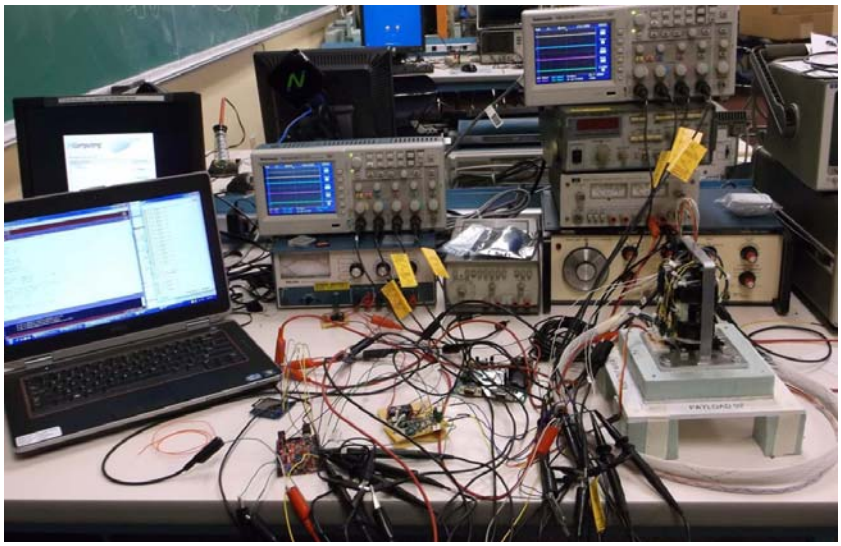

Figure 3. Setup for lab testing

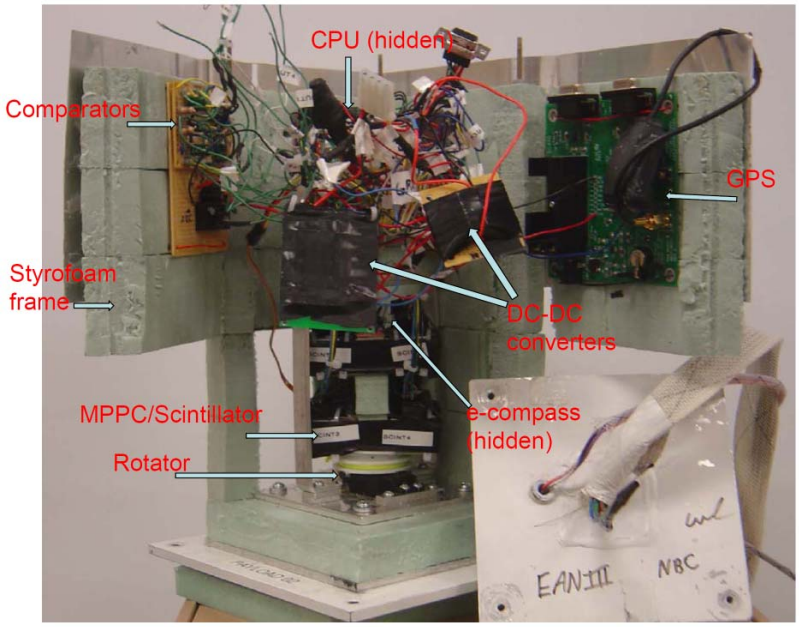

Figure 4. Interior view of GU-HARD-PL02

2.1. Detector Module

Four active detector elements are arranged in a square for detection of cosmic rays in the east-west plane. In this arrangement, two detector elements are expected to simultaneously produce an electric pulse. Each active detector element consists of a Photonique SSPM 0905V13MM silicon photomultiplier (SiPM) [2] attached via optical epoxy to a $3 \times 3 \times 1\ cm^3$ CsI(TI) scintillating crystal, as shown in Figure 5(a). To artificially supply lights to the scintillator for lab testing purposes, a green LED is also attached to the scintillator. As a charged particle traverses the scintillator, light is emitted. The SiPM then converts this light into an electric pulse. The scintillators are wrapped in Teflon tape to reflect stray photons back in, increasing the number of photons detected by the SiPM, and then in electrical tape to block outside light. A wrapped scintillator is shown in Figure 5(b). Each SiPM is connected to a pre-amplifier, also visible in the photos. The pre-amplifier generates a negative pulse with a magnitude ranging from 0 to about -1.0V depending on the number of photons impinging on the SiPM. The advantage of using SiPMs over traditional photomultiplier tubes (PMTs) is that they only require a very low (~30V) bias voltage, as opposed to the ~1 kV require by PMTs. This eliminates the need to pot the electronics in a dielectric, which is required with PMTs in near vacuum applications.

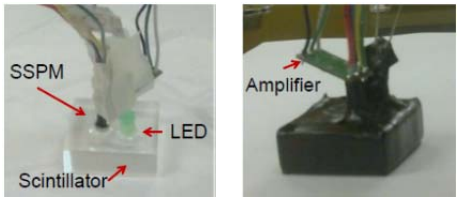

(a) (b)

Figure 5. Detector module: (a) photo diode and scintillator (b) integration with a preamplifier

One challenge of working with the SiPM units is that the signals generated are very short, e.g., peak sensitivity wavelength = 680 nm [2]. The pre-amplifiers had a typical rise time of 5 ns, although the long decay time of the CsI(TI) crystal resulted in pulses with a width on the scale of 1 µs. To detect such short pulses requires fast electronics. An application circuit of the pre-amplifier used for the detector module is shown in Figure 6 where capacitors C1 and C2 have a typical value of 10 nF.

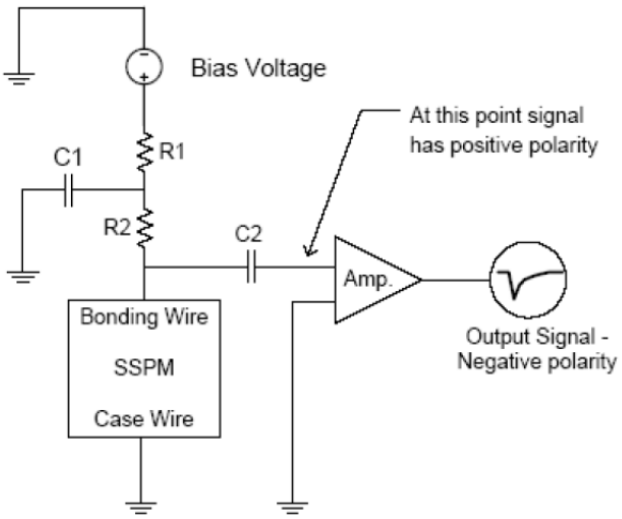

Figure 6. Application circuit diagram of the pre-amplifier for SSPM [3]

In order to detect the east-west asymmetry, the detector must be oriented so that the scintillator lies in the east-west plane. Given that the HASP instrument rotates during the flight, an HMC6352 electronic compass [4] is used to determine the orientation of the detector module. When the orientation of the payload drifts more than 10° from the desired orientation, a servo motor is used to adjust the detector. The completed detector module with the rotator module is shown in Figure 7.

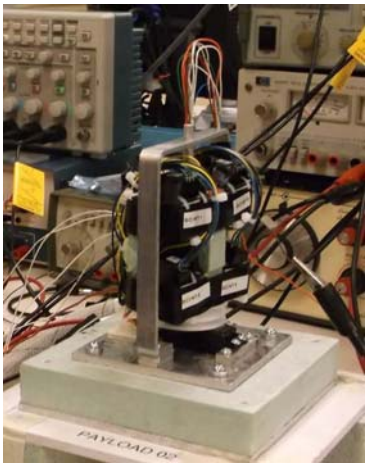

Figure 7. Fully assembled detector module with the rotator module

2.2. Comparator Module

Each SiPM unit outputs a voltage proportional to the number of detected photons. However, this voltage signal is small and negative. This signal is inverted and amplified by an AD8616 inverting OP amp with a high voltage gain and large bandwidth operating at a frequency of up to 20 MHz [5]. Typical LM741 OP amp was first tried but did not work due to the requirement of a high gain at high frequencies.

2.3. Coincidence Detector

The output of the comparator module is connected to the digital inputs of the microprocessor. To monitor for a coincidence in two or more SiPM modules at a time, the microprocessor polls these inputs approximately once each microsecond. When this condition is met, the SiPM modules that contributed to the coincidence are identified and stored for later analysis by.

2.4. Microprocessor/CPU

A chipKIT Uno32 Prototyping Platform [6] is used as the main microprocessor module. This board provides a number of functions, including poling the digital I/O pins to determine whether a coincidence has been met; serial communication with HASP; monitoring temperature, detector orientation and GPS time; controlling the servo to adjust detector orientation; and recording data to an SD card.

The following programming codes were implemented for the necessary functionality:

- FlightCode.pde: Main program to integrate all subroutines and download the codes onto the microcontroller
- M01_GPS.pde: for GPS-related functions
    - void SetupGPS()
    - void GetOnboardGPSString()
    - void GetGPSTime(char *str, unsigned int size, char *time)
    - void ParseGPSString(unsigned char *str, unsigned int size)
- M02_RadDet.pde: for radiation detection-related functions
    - void SetupRadDet()
    - int GetHit()
- M03_SDmemory.pde: for memory card-related functions
    - void SetupSD()
    - int GetFilename()
    - void WriteEvent()
    - void Reboot()
- M04_Servo.pde: for control of a servo motor
    - void SetupServo()
    - void PointNorth()
    - int ControlServo(float heading)
    - void ServoRotate(Servo *s, float angle)
    - inline float MicrosecondsToAngle(float micro)
    - inline float CheckAngle(float angle)
- M05_eCompass.pde: for electronic compass-related functions
    - void SetupECompass()
    - float GetHeading()
    - void CalibrateCompass()
- M06_HASPSerial.pde: for serial communication-related functions
    - void ReadHASPSerial()
    - void SendHASPSerial()
- M07_TempSensor.pde: for temperature sensor-related functions
    - float GetTemp()

All of these codes were thoroughly tested in the lab and implemented into the microcontroller. During integration, however, it was discovered that the serial port on the Uno32 was using TTL logic levels, whereas the HASP equipment required RS-232 logic levels. In order to enable serial communication, a MAX233 line driver/receiver was additionally installed. After installation, commands could be sent to the

payload successfully and science and housekeeping data were received by the HASP instrument, both during integration and flight.

2.5. Power Module

Most of the onboard modules require a 5Vdc supply to operate, particularly the microprocessor, GPS, SiPM pre-amplifiers, temperature sensor, and rotator. To provide this voltage, a Murata NDY2405C DC-DC converter is used [7]. The e-compass and SD card both required a 3.3V supply, which was provided by the Uno32's built-in, regulated 3.3V supply. The comparator (high gain, large bandwidth OP amp) requires a dual power supply with a maximum differential voltage of 6V. As a result of considering all constraints, a ±2.5V supply is used [8].

Another consideration is the sensitivity of the SiPM gain to the bias voltage. Initially, the HASP 30V power was supplied to the SiPM. However, it was discovered during the HASP instrument integration that the HASP 30 V power supply, which was being used without regulation as the bias voltage for the SiPM units, varied over too wide a range for the SiPM to operate properly. At the upper end of the voltage range (around 32 V), the bias voltage supplied to the SiPM was sufficient to cause continuous triggering on dark noise. This issue was resolved during integration by using an RS-2415DZ regulated DC-DC converter [9], which output a stable ±15Vdc over an 18-36V input range. For the required single power supply, this ±15Vdc dual power supply was wired to produce a 30V single DC output.

3. Numerical Results and Discussions

3.1. Lab Testing Data – Detector and Comparator Modules

For a proper operation of the detector module, selection of properly operating SiPMs was a critical task. As such, one of the key test data was the bias voltage of the SiPM, as well as the output signal from the pre-amplifier. In reference to Figure 6, after assembling a green LED/scintillator and a pre-amplifier as a detector module under test, the output voltage of the pre-amplifier was measured. Table **1** shows two test data for 4 detector modules (determined to be properly functioning) among 12 detector modules tested. Test 1 was to determine the maximum possible output from the preamplifier which operates with a 5Vdc power supply. Test 2 was to determine a proper bias voltage for the SiPM on the pre-amplifier board.

Figure 8(a) shows an actual pre-amplifier output when all subsystems of the payload were integrated. As shown, the pulse period was about 1.8 μs while its amplitude was 640 mV (not shown). Figure 8(b) shows the comparator output corresponding to the pre-amplifier output. The high gain, high bandwidth OP amp for the comparator was able to successfully process the short negative pulse from the pre-amplifier and produced a positive pulse of a similar same duration with its amplitude of ~2.5V. The output of 2.5V was expected as the use of ±2.5V dual power supply was used and also the OP amp has internally a configuration of a push-pull class B amplifier. As the comparator output is supplied to the micro-controller

operating based on TTL logic (i.e., 0 ~ 3.3 Vdc) with a threshold voltage of 2.4 Vdc. The +2.5 V output was a proper output level for the logical operation of the micro-controller.

Table 1. Testing Data of the Detector Module

Pre-amp board #	**Test 1**	**Test 2**
	Preamp Max. Output Voltage [V]	**SiPM Bias Voltage [V]**
	Test condition: Preamplifier input: a 100 kHz pulse signal coupled by C2 = 10 µF; SiPM is not powered (i.e., OFF)	**Test condition**: Preamplifier output: at negative peak voltage < -1V
#4	-2.56	28.2
#5	-2.56	26.2
#8	-2.40	27.6
#10	-2.72	28.0

3.2. In-Flight Experimental Data

GU-HARD-PL02 was flight-certified after a 2nd attempt to pass the thermal vacuum testing at the CSBF site. The in-flight data shown in Figure 9~Figure 13 was gathered during the HASP 2012 flight through the serial communication to the HASP data repository on the ground in real time.

Figure 9 shows the temperature inside the payload. The temperature was monitored to ensure all

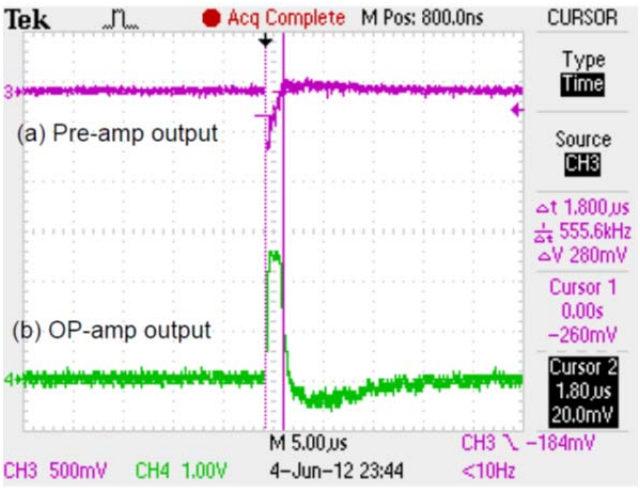

Figure 8. Output signals: (a) pre-amplifier (b) OP amp (comparator)

subsystems of the payload were in operating temperature range during both the thermal vacuum testing and HASP flight. As shown, the temperature was in the range of -20 °C ~ +38 °C except for one data point which shows a temperature of 233 °C (from raw data). As the inside temperature would be cooling by itself so rapidly at the time instant for the next data point, it is assumed that the data might be corrupt during the serial transmission somewhere between the micro-processor serial port and the ground receiver.

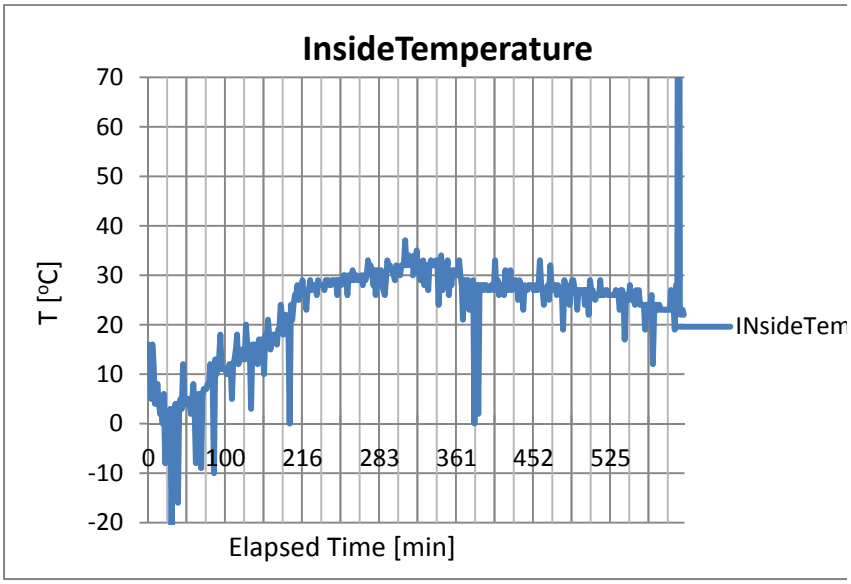

Figure 9. Temperature inside the payload

Figure 10 shows the payload orientation in reference to the East-West (E-W) line. The electronic compass inside the payload was initially oriented along the E-W line such that any angular deviations from the reference orientation were captured and the rotator module could reverse the rotation in the opposite direction. The angular correction was done with a deviation threshold of 10 degrees in either clockwise (negative) or counter-clockwise (positive) direction. As shown, the payload lost its E-W orientation at some points (e.g., near 361 minutes) but was able to re-align its orientation within the intended orientation error of ±10 degrees. However, sudden changes in angular orientation, e.g., 167 degrees and then 185 degrees (plotted as -175 degrees in the figure) are subject to further investigation to determine whether the HASP really rotated by that much, or it was due to a malfunctioning of the

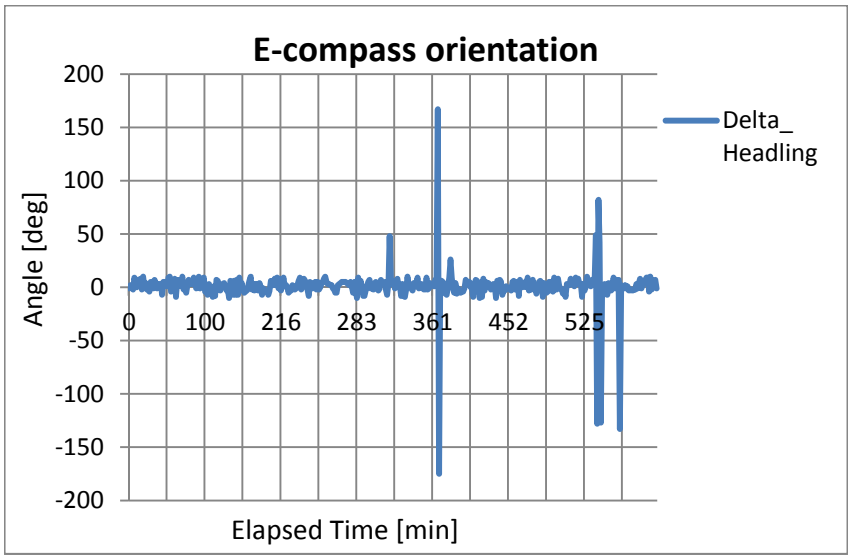

Figure 10. Orientation angle [degrees] of the electronic compass referenced to the East-West

rotator module (e.g. over-correction).

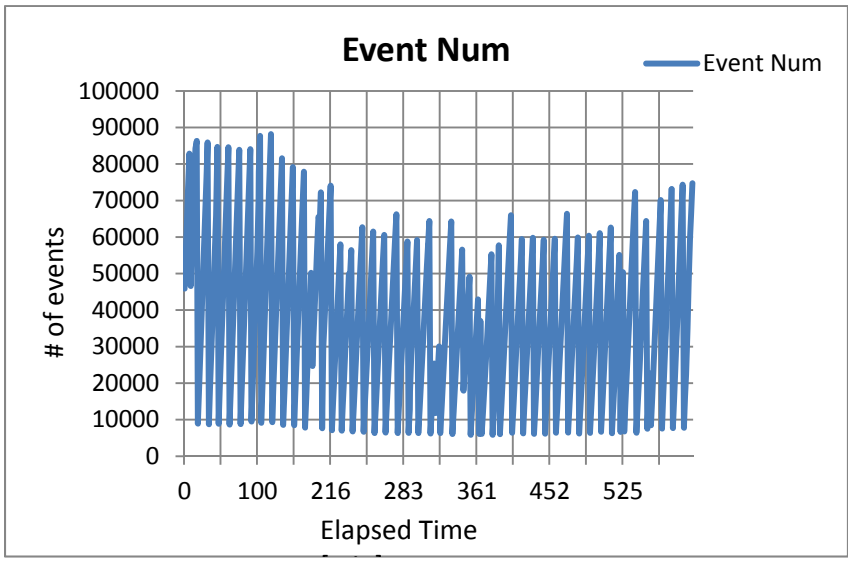

Figure 11. Number of coincidence events counted by the Coincidence Module

Figure 11 shows the cumulative event numbers of coincidences. An event is declared when the input voltage to a designated pin of the micro-controller is HIGH, which is ideally a signal when an SiPM produces a electric pulse due to arrivals of cosmic rays in a direction. As shown in the figure, there are so many events per minutes, ranging from ~6,000 to ~86,000. Furthermore, ideally, the event numbers would be monotonically increasing as the total number of events is accumulating all events occurred in time. Obviously, something happened in the micro-controller inside the payload on the HASP as this fluctuation of numbers could only happen when the micro-controller regularly resets the event number. The most logical explanation is that the microcontroller rebooted itself approximately every 7 minutes, a failure mode not observed in the lab.

Figure 12 shows the hit rates (or event rates), defined as the number of events of coincidence per minute. An expected range of events was somewhere between 10~20 per minutes. These event numbers were in the expected range during two preliminary integration tests performed on the integraton emulator in the CSBF lab. This was also the reason of declaring a failure to pass the 1st thermal vacuum test on the HASP. The payload passed the thermal vacuum test in the 2nd attempt after somewhat unrelated improvement (i.e.,

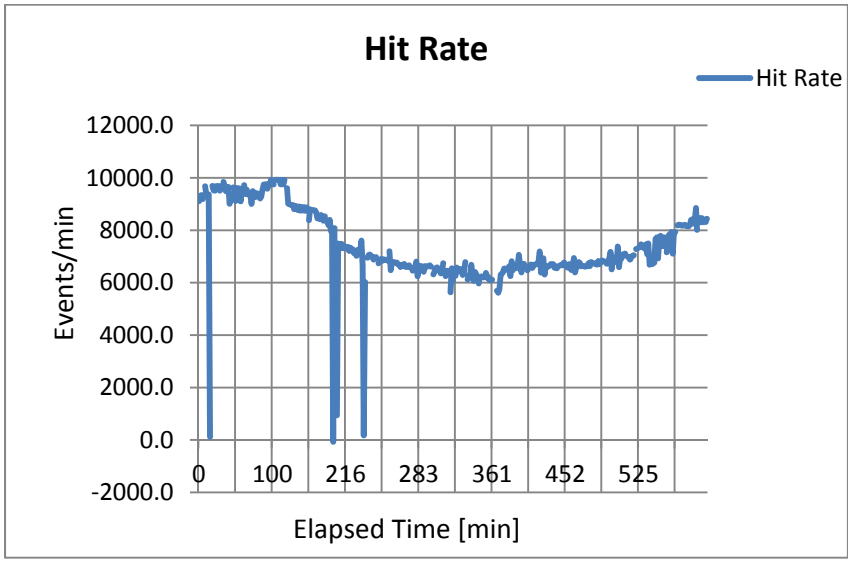

Figure 12. Coincidence rate [Events per minute] in all directions

addition of an 18~30V-in-30V-out DC-DC converter in preparation for possible drops in the supply voltage level from the HASP 30V power supply after a few hours of flight), and the event numbers were in the expected range during the 2nd thermal vacuum test.

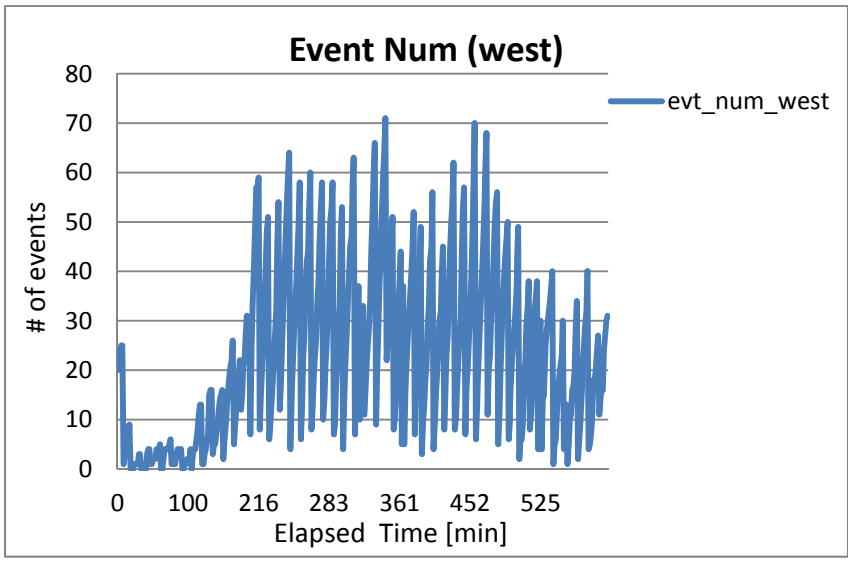

Figure 13. Coincidence rate [Events per minute] in East-West direction

Similarly, Figure 13 shows a similar trend of numbers fluctuating as in Figure 11 as the calculation was derived from the total number of events. However, this figure does indicate that there are substantially less number of E-W events compared to the all events from all angular directions.

4. Failure Mode and Effect Analysis

For potential failure modes on technical aspects, some basic concepts of the well-known failure mode and effect analysis (FMEA)[1] can be applied to the payload "system design." As such, rather than tabularizing various factors for the analysis and corrective actions to be taken, as it would be done in a formal FMEA, we provide qualitative assessment for further investigation of the possible causes of the subsystem malfunctioning/failure.

Pin-pointing an exact cause is difficult because the failure is not reproducible in the lab. However, based on the observations of experimental data, we assess the potential causes of the problems as follows, and they will be the focus of further improvement of the payload functionality for future flights and in-flight experiments.

SiPM - During the first thermal vacuum test, the detector malfunctioned, essentially triggering continuously. To help resolve this issue, the 18~30V DC-DC converter, described above, was installed and seemed to resolve the problem, as the detector functioned as expected during the second thermal vacuum test and during the pre-flight instrument test. However, for reasons that are still uncertain, the

[1] Only basic concepts of the FMEA are applied to quickly determining key potential failure modes without calculating Risk Priority Numbers (RPNs) from a full FMEA.

instrument returned to the failure mode observed during the first thermal vacuum test during flight. No usable data was returned from the detector module. It is suggested that the bias threshold shown in Table **1** may need to be set lower (or higher) as a threshold of ~29V (and slightly adjusted for individual SiPMs by a series of resistors-based voltage divider circuit) was used for the detector module in GU-HARD-PL02 to produce strongest pulses from all SiPMs. A lower or higher bias voltage would produce a weaker pulse that prevents a false triggering of the comparator module.

Comparator - The output of the pre-amplifier of the detector module is input to a comparator. Although the original design suggested the comparator voltage be adjustable via an external command, the threshold voltage for the comparator is set to 0 V as it provided adequate results in the lab. Adjusting it to a non-zero threshold had yielded weaker output voltages (less than the desired 2.4 V for TTL logic) from the class B amplifier inside the OP amp for the comparator. As a possible cause of ultimate false event declaration, the application circuit and the circuit board of the comparator would need more attention to remove any design flaws around it.

Micro-controller - The microprocessor functioned as expected during flight, except that somehow the event numbers were reset regularly by itself. Data were returned to the ground at the expected rate of serial communication, and the temperature and detector orientation remained within expected values most of the time. The GPS timestamp from the onboard GPS was also received, although the GPS timestamp from the HASP instrument was not. However, since the onboard GPS functioned properly, the HASP GPS timestamp was not required. There was a problem with the onboard SD card, however. During shipment, it seems to have jostled out of place, despite being taped into position. Thus, events were not recorded to the SD card during flight. However, the data received via HASP downlink provided redundancy, thus this failure had very little impact on flight success. It is suspected that the overall connections of the subsystems might have caused undesirable triggering pulse to reset the operation of the coincident detector, and/or more attention could be given to the micro-controller codes for more aggressive prevention of unexpected triggering/operation.

Power module – the overall ground level was somewhat unstable, especially when the rotator operates, or a large amount of cosmic rays arrive, resulting in a large peak, e.g., more than -1.0V, at the pre-amplifier output of the detector module. All DC-DC converters would need to be revisited to ensure each of them could cope with an unexpected drawing of a certain level of excessive current from the DC-DC converter.

5. Participants

There were six undergraduate students from ECE department. All seniors were involved from the beginning of the project in Fall 2011, and sophomores joined the team during Fall 2011 or in the beginning of Spring 2012. One graduate student was recruited to help the team for a shorter period of time during the summer 2012. This student team was advised by two faculty members as shown below.

Student team members

Name	Major/Concentration	Year (as of Spring '12)	Gender	Ethnicity
Emily Wright	Electrical & Electronics	Senior	Female	White
Robert Frantz	Electrical & Electronics	Senior	Male	White
Daniel Grasinger	Computer Engineering	Senior	Male	White
Joe Veneri	Electrical & Electronics	Sophomore	Male	White
Nichole McGuire	Electrical & Electronics	Sophomore	Female	White
E. Aaron Neiman	Computer Engineering	Sophomore	Male	White
Sriharsha Kotte	Electrical Engineering	Graduate student	Male	Asian

Faculty advisors

Name	Title	Department	Gender
Dr. Wookwon Lee	Associate Professor	Electrical & Computer Engineering	Male
Dr. Nicholas Conklin	Assistant Professor	Physics	Male

6. Presentations and Publications

- Robert Frantz, Dan Grasinger, and Emily Wright, "High Altitude Radiation Detection", presented at IEEE Region 2 Student Activities Conference, Columbus, OH, April 2012.
- W. Lee and N. Conklin, "High Altitude Radiation Detector (HARD): Integration of Undergraduate Research into Senior Design and Lessons Learned ", abstract accepted, 2013 ASEE Annual conference, June 2013.

7. Concluding Remarks

Although the payload failed to collect the desired cosmic-ray data, all other parts of the design, including serial communications, payload orientation, and temperature monitoring, functioned as expected. Additionally, this project provided student team members with an engineering opportunity that requires technical and also non-technical skills to solve real-world problems. This project was adopted as a senior design project for the 2011-2012 academic year at Gannon with three of the design team members

participating as seniors in the ECE department. Therefore, despite the lack of science data, this project was a considerable success from a student education standpoint.

The Gannon team plans to revise the payload design, fixing the potential sources of failure outlined above, and launch its own small-scale balloon system to carry this payload to the near space. Another payload, so called GU-HARD-PL03, will also be developed during this period to try again (if accepted) on the HASP 2013 flight.

References

[1] Gannon University HARD project team, "High Altitude Radiation Detector (GU-HARD-PL02)," *HASP 2012 proposal submitted to the HASP 2012 Program*, 12/16/2011.

[2] Photoniques SA, *1.3mm^2 active area, low noise solid state photomultiplier for visible and near-IR light applications*, Data sheet, Doc. No.: SSPM_0905V13MM, Sept. 2009.

[3] Application circuit diagram for AMP-0604 and AMP-0611, Photoniques SA, available on line at http://www.photonique.ch/Prod_AMP_0600.html.

[4] Honeywell, *Digital Compass Solution HMC6352*, data sheet, available on line at https://www.sparkfun.com/products/7915.

[5] Analog Devices, *AD8615/AD8616/AD8618: Precision, 20 MHz, CMOS, Rail-to-Rail Input/Output Operational Amplifiers*, data sheet, 2008.

[6] Digilent, *chipKIT™ Uno32™ Board Reference Manual*, Doc: 502-209, October 25, 2011.

[7] Murata NDY2405C, *NDY Series: Isolated 3W Wide Input DC/DC Converters*, data sheet, Doc. No.: KDC_NDY.F02, 2012.

[8] Emerson Network Power, ASA03G24-L-ND, *18-36VDC to 2.5V@3A Converter*, data sheet, rev. 01.30.08, Jan. 2008.

[9] Recom Power, RS-2415DZ, *ECONOLINE DC/DC-Converter*, REV: 0/2012.